bioRxiv preprint doi: https://doi.org/10.1101/155002; this version posted June 28, 2017. The copyright holder for this preprint (which was not certified by peer review) is the author/funder, who has granted bioRxiv a license to display the preprint in perpetuity. It is made available under aCC-BY-NC-ND 4.0 International license.

Melanism patches up the defective cuticular morphological traits through promoting the up-regulation of cuticular protein-coding genes in *Bombyx mori*

Liang Qiao[*1], Ri-xin Wang[§], You-jin Hao[*], Hai Hu[§], Gao Xiong[§], Song-zhen He[§], Jiang-bo Song[§], Kun-peng Lu[§], James Mallet[†], Ya-qun Xin[‡], Bin Chen[*], Fang-yin Dai[§1]

***** Chongqing Key Laboratory of Vector Insects, Institute of Entomology and Molecular Biology, College of Life Sciences, Chongqing Normal University, Chongqing, 401331, China

[§] State Key Laboratory of Silkworm Genome Biology; Key Laboratory of Sericultural Biology and Genetic Breeding, Ministry of Agriculture; College of Biotechnology, Southwest University, Chongqing 400716, China.

† Department of Organismic and Evolutionary Biology, Harvard University, Cambridge, MA 02138, USA

‡Department of Evolutionary Ecology, LMU Munich Großhaderner Str. 2, 82152, Germany

bioRxiv preprint doi: https://doi.org/10.1101/155002; this version posted June 28, 2017. The copyright holder for this preprint (which was not certified by peer review) is the author/funder, who has granted bioRxiv a license to display the preprint in perpetuity. It is made available under aCC-BY-NC-ND 4.0 International license.

Running title: Role of melanin on cuticle defects

Keywords: Melanic coloring; Cuticle features; Cuticular protein-encoding genes; Induction; *Bombyx mori*

[1] **Corresponding Authors:**

Liang Qiao, Chongqing Key Laboratory of Vector Insects, Institute of Entomology and Molecular Biology, College of Life Sciences, Chongqing Normal University, No. 37 Daxuecheng Road, Chongqing, 401331, China; E-mail: qiaoliangswu@163.com; Tel: 86-23-65910315

Fang-yin Dai, State Key Laboratory of Silkworm Genome Biology, Key Laboratory for Sericulture Functional Genomics and Biotechnology of Agricultural Ministry, Southwest University, No. 2 Tiansheng Road, Chongqing, +86-23-68400715, China; E-mail: fydai@swu.edu.cn; Tel: 86-23-68250346

bioRxiv preprint doi: https://doi.org/10.1101/155002; this version posted June 28, 2017. The copyright holder for this preprint (which was not certified by peer review) is the author/funder, who has granted bioRxiv a license to display the preprint in perpetuity. It is made available under aCC-BY-NC-ND 4.0 International license.

Abstract

Melanin and cuticular proteins are important cuticle components in insect. The cuticle defects caused by the loss function of cuticular protein-encoding genes could hinder melanin deposition. However, the effects of melanin variation on cuticular protein-encoding genes and the corresponding morphological traits associated with these genes remain largely unknown. Using *Bombyx mori* as a model, we showed that the level of melanism during larval cuticle pigmentation correlated positively with the expression of cuticular protein-encoding genes. This correlation stemmed from the simultaneous induction of these genes by the melanin precursors. More importantly, the effect of the melanism background on the cuticle induced the up-regulation of other functionally redundant cuticular protein-encoding genes to rescue the morphological and adaptive defects caused by the dysfunction of some mutated cuticular proteins, and the restorative ability increased with increasing melanism levels, which gives a novel evidence that melanism enhances insect adaptability. These findings deepen our understanding of the interactions among cuticle components, as well as their importance in the stabilization of the normal morphology and function of the cuticle.

Introduction

The prerequisite for the benefits of melanism to insect is not only the integrity of the melanin biosynthesis and regulatory pathway (Wilson *et al.* 2001; Liu *et al.* 2015; Mallet and Hoekstra 2016), but also the normal presence of the platform it relied on

bioRxiv preprint doi: https://doi.org/10.1101/155002; this version posted June 28, 2017. The copyright holder for this preprint (which was not certified by peer review) is the author/funder, who has granted bioRxiv a license to display the preprint in perpetuity. It is made available under aCC-BY-NC-ND 4.0 International license.

(Wittkopp *et al.* 2003; Wittkopp and Beldade 2009; Andersen 2010; Moussian 2010; Van Belleghem *et al.* 2017). For the insects, the most important fundamental platform for the color pattern drawing is the cuticle (Hopkins and Kramer 1992; Andersen 2010; Moussian 2010). During shaping the cuticle, the maintenance and stability of the cuticle features depends on normal functional cuticular proteins and the interactions with other components (Hopkins and Kramer 1992; Guan *et al.* 2006; Suderman *et al.* 2006; Andersen 2010; Moussian 2010; Chaudhari *et al.* 2011; Noh *et al.* 2016). Due to the crucial roles of cuticular proteins on cuticle development, when their coding genes are loss of function, the abnormal or defective cuticle will likely affect the deposition and attachment of melanin, which is not conducive to the performance of color pattern (Kanekatsu *et al.* 1988; Oota and Kanekatsu 1993; Arakane *et al.* 2012; Jasrapuria *et al.* 2012; Wang 2013; Noh *et al.* 2015). Yet little is known about the corresponding response mode of cuticular protein-encoding genes via the alteration of the melanin biosynthesis or regulatory pathway.

Recently, several high throughput expression surveys showed that the abundance of cuticular protein-encoding genes in different colored integuments varied in some insect species, especially with evidently up-regulated in the melanic regions (Futahashi *et al.* 2012; He *et al.* 2016; Wu *et al.* 2016; Tajiri 2017), and some of those shared very similar expression patterns and functions (Nakato *et al.* 1994; Nakato *et al.* 1997; Shofuda *et al.* 1999; Okamoto *et al.* 2008; Liang *et al.* 2010; Tang *et al.* 2010; Qiao *et al.* 2014).These studies implied that there are probably some relationships between the promotion of melanism and the expression of cuticular

bioRxiv preprint doi: https://doi.org/10.1101/155002; this version posted June 28, 2017. The copyright holder for this preprint (which was not certified by peer review) is the author/funder, who has granted bioRxiv a license to display the preprint in perpetuity. It is made available under aCC-BY-NC-ND 4.0 International license.

protein-encoding genes. Prior to this study, further exploring and understanding of the potential relationships were unclear. Additionally, when melanism-promoting instructions and defective cuticle proteins occur simultaneously, what are the effects of their relationships on the presence of the corresponding morphological traits ?

In the Lepidoptera model, *Bombyx mori*, an intriguing phenomenon has been reported that a larval melanic mutant, *Striped* (p^S, 2-0.0) is able to rehabilitate the malformed body shape, as well as the adaptability defects of the *stony* mutant (*st*, 8-0.0) (Xiang 1995; Banno *et al.* 2005). A recent study clarified that a transcription factor, *Apontic-like*, which boosts the expression of melanin synthesis genes in epidermal cells, is responsible for the p^S mutant (Yoda *et al.* 2014). Besides this, there are also multiple alleles with different melanism degrees at the *p* locus, including p^B, p^M, *etc* (Xiang 1995; Banno *et al.* 2005; Yoda *et al.* 2014). And the *stony* mutant (*st*, 8-0.0) which precisely caused by the deletion of a RR1-type larval cuticular protein-encoding gene, *BmLcp17* (or *BmorCPR2*) showed hard and tight touch feeling, uncoordinated ratios of the length of the internodes and the intersegment folds (I/IF), bulges at intersegment folds, and severely defective locomotion and behavioral activities in the larval stage (Qiao *et al.* 2014). In addition, the similarity of the gene expression patterns and functional characteristics among some members of the RR1-type larval cuticular protein-encoding gene family, such as *BmLcp18*, *BmLcp22*, *BmLcp30* also suggest that they may play very similar roles as *BmLcp17* in shaping the larvae cuticle (Nakato *et al.* 1994; Nakato *et al.* 1997; Shofuda *et al.* 1999; Okamoto *et al.* 2008; Liang *et al.* 2010; Tang *et al.* 2010; Qiao *et al.* 2014). These

bioRxiv preprint doi: https://doi.org/10.1101/155002; this version posted June 28, 2017. The copyright holder for this preprint (which was not certified by peer review) is the author/funder, who has granted bioRxiv a license to display the preprint in perpetuity. It is made available under aCC-BY-NC-ND 4.0 International license.

dispersed findings are linked through the epistasis of p^S to *stony*, then provide the breakthrough and the exceptional genetic resources for exploring the interactions between melanin and cuticular protein-encoding genes.

Here we illustrated that the transcripts levels of four cuticular protein-encoding genes were positively correlated with the melanism degree of larval cuticle, which were due to the simultaneous induction these genes by the intracellular melanin precursors. Moreover, by importing melanism-promoting instruction into the *stony* mutant, the cuticle deficiency rescued through functionally redundant compensation by some other up-regulated cuticular protein-encoding genes, which a new evidence that melanism as a beneficial trait. These findings deepen our understanding of the interactions among genetic factors which shape morphological features in lepidopteran, and emphasize the ecological and evolutionary significance of these mutual interactions.

Materials and Methods

Silkworm strains

Wild-type strains Dazao ($+^p$) and melanic mutant strains p^M, p^S and p^B (Xiang 1995; Banno *et al.* 2005; Yoda *et al.* 2014) were analyzed in this study. The darkness of pigment was measured as mean OD value using Image J (https://imagej.nih.gov/ij/). In terms of melanism degree, the body color of an individual that is homozygous at one of the aforementioned melanic loci is darker than that of a heterozygous individual (Xiang 1995; Banno *et al.* 2005). The albinism mutant *albino* (*al*) (Banno

bioRxiv preprint doi: https://doi.org/10.1101/155002; this version posted June 28, 2017. The copyright holder for this preprint (which was not certified by peer review) is the author/funder, who has granted bioRxiv a license to display the preprint in perpetuity. It is made available under aCC-BY-NC-ND 4.0 International license.

et al. 2005; Fujii *et al.* 2013), non-diapause wild-type strain N4 (used for melanin inhibition treatment) and *BmLcp17* deletion strain Dazao-*stony* (near isogeneic line of Dazao, which have been backcrossed with Dazao over 26 generations) were supplied by the Silkworm Gene Bank in Southwest University. The *al* mutant was fed with artificial die at 28℃, and the others were fed fresh mulberry leaves under a 12 h/12 h light/dark photoperiod at 24 °C.

Chemicals and cell lines

L-dopa (D9628), dopamine (H8502), tetrahydrofolic acid (BH_4) (T3125) and 2,4-Diamino-6-hydroxypyrimidine (DAHP) (D19206) were purchased from Sigma-Aldrich (St. Louis, MO, USA). *BmNs* cell line was kept in our laboratory.

Mating combinations and progeny phenotypes identification

The p^S and p^M strains were crossed with the Dazao-*stony* strain to generate the F_1 generation, respectively. The F_2 generation were produced by an F_1 self-cross, and individuals of day 5 of the fifth-instar were collected to further use. The p^B strain was crossed with the Dazao-*stony* strain to generate F_1 progeny, which mated with the Dazao-*stony* strain to generate the BC_1 generation, and fed them until at day 5 of the fifth-instar. Firstly, individuals of the F_2 or BC_1 generations were separated by their cuticle pigmentation. Subsequently, their phenotypes were further classified by morphological characteristics, touch feeling, and the ratios between the number of internodes and intersegmental folds in the second, third, and fourth abdominal segments based on a earlier method (Qiao *et al*. 2014).

Genotyping

bioRxiv preprint doi: https://doi.org/10.1101/155002; this version posted June 28, 2017. The copyright holder for this preprint (which was not certified by peer review) is the author/funder, who has granted bioRxiv a license to display the preprint in perpetuity. It is made available under aCC-BY-NC-ND 4.0 International license.

Because the p^S, p^M and p^B mutations are multiple alleles at the *p* locus, they should be located in proximity each other on the chromosome 2 (Xiang 1995; Banno *et al.* 2005; Yoda *et al*. 2014). Based on the reported sequence of the gene corresponding to the p^S allele, a polymerase chain reaction (PCR)-based molecular marker within of the genomic region of the *Apontic-like* was designed. PCR screening were performed in the p^X (*X*=*M*, *S* and *B*) and Dazao-*stony* to obtain the polymorphism molecular marker for *p* locus. Similarly, molecular marker was also designed within genomic region of the *BmLcp17* for polymorphism screening of the *stony* locus. The primers used in this study are listed in Table S1.

Association analysis of gene expression, phenotype and genotype

Day 5 fifth-instar larvae of the Dazao or Dazao-*stony* strains were selected for cuticle dissection. The cuticles of the semi-lunar marking region and the non-melanic portion between the paired semi-lunar marking were finely dissected. Then, gene expression levels of *BmLcp17*, *BmLcp18*, *BmLcp22* and *BmLcp30* in these regions were compared. Gene expression patterns in the dorsal epidermis of abdominal segments (from semi-lunar marking to star marking) from day 5 of fifth instar larvae (Dazao, p^S/+, p^M/+, p^B/+). Similarly, day 1 of second instar larvae of the *al* and Dazao strains were also investigated. In addition, the same regions of dorsal epidermis were collected from F_2 generation individuals with the p^S/p^S, *st/*st, and p^S/+, *st/st* genotypes, as well as the p^M/p^M, *st/st* and p^M/+, *st/st* genotypes for gene expression analyses. For all genotyped individuals, the ratios of the length of the intersegment and the intersegment fold were also analysed using image J.

bioRxiv preprint doi: https://doi.org/10.1101/155002; this version posted June 28, 2017. The copyright holder for this preprint (which was not certified by peer review) is the author/funder, who has granted bioRxiv a license to display the preprint in perpetuity. It is made available under aCC-BY-NC-ND 4.0 International license.

Melanin precursors-promoting and inhibition treatments

The preparation and concentration of L-dopa and dopamine solutions were slightly modified according to the description by Futahashi (Futahashi and Fujiwara 2005), and filtered with a 0.22 μm filter prior to use. Cells were washed three times with Grace medium without melanin precursors to remove metabolites and other contaminants on the cell surface. Then, 0.8mL medium containing L-dopa or dopamine was added separately into each well, and the medium without melanin precursors was used as the control. The plate was sealed with tape, wrapped with foil and incubated at 28℃ for 24 h for a gene expression analysis. In BH_4 feeding assays, the 30mM working solution was prepared by dissolving tetrahydrofolic acid into ddH_2O, and then smeared on the artificial diet to feed the *al* mutant, and ddH_2O was used as the control. Phenotype were observed and recorded from the second instar and the expression of cuticular protein-encoding genes was also analysed. For the melanism-inhibition experiment, the wild-type strain N4 was selected. Newly-hatched larvae were divided into treatment and control groups. Individuals in the treatment group fed with DAHP dissolved in 0.1M NaOH (15g/L), and individuals in the control group fed 0.1M with NaOH. Phenotypes observation and gene expressions detection were performed on day 1 of the second-instar larvae.

Quantitative RT–PCR

Total RNA extraction, reverse transcription and qRT-PCR conducted as described previously (Qiao *et al*. 2014). Three biological replicates were prepared for each condition, and *BmRPL3* was used as the internal control. Primers are listed in Table

bioRxiv preprint doi: https://doi.org/10.1101/155002; this version posted June 28, 2017. The copyright holder for this preprint (which was not certified by peer review) is the author/funder, who has granted bioRxiv a license to display the preprint in perpetuity. It is made available under aCC-BY-NC-ND 4.0 International license.

S1.

Results

Entirely distinct expression patterns of cuticular protein-encoding genes and the cuticle appearance between melanic and non-melanic regions

The expression patterns of *BmLcp17*, *BmLcp18*, *BmLcp22* and *BmLcp30* in melanic or non-melanic epidermal regions are shown in Figure 1. These results, together with earlier studies (Futahashi *et al.* 2012; He *et al.* 2016; Wu *et al.* 2016), revealed that the gene expressions were significantly higher in melanic parts of the cuticle than in non-melanic parts. Moreover, micro protrusions were more intensive in the melanic regions than in the non-melanic regions, and accompanied by a higher chitin content (another important cuticle component (Hopkins and Kramer 1992; Moussian *et al.* 2006; Andersen 2010; Moussian 2010; Chaudhari *et al.* 2011; Qiao *et al.* 2014), and the reduction chitin content was reported to impede cuticle melanism (Moussian *et al.* 2005)) (Figure S1A). These results showed that, regardless of the different genetic basis of the melanic mutants or the melanic markings in the non-melanic strains, excessive accumulation of melanin in the cuticle (accompany by the changes in the surface structure and the chitin content of the melanic cuticle) was closely related to the high expression levels of the cuticular protein-encoding genes.

Expression level of larval cuticular protein-encoding genes positively correlated with the degree of cuticle melanism

To obtain further insights into the relationships between the accumulation of

bioRxiv preprint doi: https://doi.org/10.1101/155002; this version posted June 28, 2017. The copyright holder for this preprint (which was not certified by peer review) is the author/funder, who has granted bioRxiv a license to display the preprint in perpetuity. It is made available under aCC-BY-NC-ND 4.0 International license.

melanin and the expression of cuticular protein-encoding genes, we investigated gene expression patterns using four different mutations at the *p* locus (Dazao ($+^p$), p^M, p^S and p^B), which showed gradually increasing melanin accumulation (Figure 2A). Our results revealed that the gene expression levels were gradually and significantly up-regulated with the increase in the degree of melanism of the cuticle (Figure 2B). They further showed that the expression levels correlated positively with the degree of melanism. Thus, the quantities of cuticular proteins with similar or redundant functions could be increased greatly by the increasing the degree of melanism.

Typical stony phenotyped individuals masked after the introduction of melanic loci into the BmLcp17 defection strain

We assessed the effects of modulating the melanic background on the phenotypic defects caused by the deletion of *BmLcp17*. After mating the p^B and *stony* parental, the percentage of BC_1 individuals with melanism and the normal body shape in the backcrossed population of the p^B×*stony* cross was 52 % (290/553; and theoretically, it was 25 %), yet individuals with the melanism cuticle and *stony*-type body shape were not found (theoretically should be almost equivalent to the number of individuals with melanism cuticle and normal body shape) (Figure 3). In the cross of p^S×*stony*, ~10.8% (36/331) of F_2 progeny had an lighter melanism body color and smaller body size (Figure 3). These individuals exhibited a little hard and tight touched body, but the body was much softer than that of the *stony* mutant. Their intersegment folds bulged slightly, and the length were significantly shorter than that of the internodes; accordingly, their phenotypes slightly resembled the morphological features of the

bioRxiv preprint doi: https://doi.org/10.1101/155002; this version posted June 28, 2017. The copyright holder for this preprint (which was not certified by peer review) is the author/funder, who has granted bioRxiv a license to display the preprint in perpetuity. It is made available under aCC-BY-NC-ND 4.0 International license.

stony mutant (Figure 3 and 4A). Even so, We did not find individuals with the typical *stony*-type body shape and also defective adaptability under the melanism background (theoretical ratio is 3/16). (Figure 3). Similarly, in the p^M×*stony* corss, only approximately ~11.7% (51/437) of the individuals of the F_2 population were very lightly melanic, but they exhibited obviously unusual morphological features (Figure 3, Figure 4A). When compared with the ~10.8% F_2 individuals (aforementioned) from the p^S×*stony* cross, the touch feelings of individuals from the p^M×*stony* cross were tighter and firmer, and the intersegment folds bulged more obviously and had a higher proportion among the segments, meaning that their body features were closer to the phenotype of the *stony* mutant (Figure 3 and 4A) (Qiao *et al.* 2014). Nevertheless, melanic individuals showing the typical *stony*-type body features and defective adaptability still did not appear (theoretical ratio is 3/16) in the progeny from the p^M × *stony* cross. Therefore, induction of the melanic mutation into individuals with a defective cuticular protein-encoding gene could mask the adverse phenotypes, and the masking effect was more remarkable with the increasing degree of melanism.

Other larval cuticular protein-encoding genes up-regulated evidently in the melanic and non-stony phenotypic, but with mutated BmLcp17 genotypic offspring

Using the molecular markers (closely linked to the *p* and *st* loci, respectively), we further genotyped the progenies with melanic color pattern and non-*stony* (including ambiguous *stony*-like) body shape. The results revealed that approximately 49% of the individuals showing a melanic color and normal body shape in the BC_1 population from the p^B×*stony* cross was the $p^B/+^{pB}$, *st/st* genotype (Figure 4A). The ratios of the

bioRxiv preprint doi: https://doi.org/10.1101/155002; this version posted June 28, 2017. The copyright holder for this preprint (which was not certified by peer review) is the author/funder, who has granted bioRxiv a license to display the preprint in perpetuity. It is made available under aCC-BY-NC-ND 4.0 International license.

length of the internodes and the intersegment folds (I/IF) were ~4, which is very similar to that in $p^B/+^{pB}$, $+^{st}/st$ individuals, and also no significant differences as that in the wild-type individuals (Figure 4B) (Qiao *et al*. 2014). In the F_2 generation from the p^S×*stony* cross, approximately 9.3% of the individuals with the p^S/p^S, *st/st* genotype and very few individuals (~1%) with the genotype $p^S/+^{pS}$, *st/st* exhibited a melanic color and the normal body shape (Figure 4A). For p^S/p^S, *st/st* genotyped individuals, the I/IF value was approximately 3.3 (Figure 4B). Although the I/IF value was lower than that in p^S/_, $+^{st}$/_ individuals (approximately 4, Figure 4B), it was much higher than that in the *stony* mutant (approximately 1.6 (Qiao *et al*. 2014)). Despite the slightly smaller body size of the p^S/p^S, *st/st* individuals, their body shape was essentially normal (Figure 4A). The genotypes of those lightly melanic individuals, whose body shape was slightly like that of the *stony* phenotype (mentioned in Result 3), were all the $p^S/+^{pS}$, *st/st*, and the I/IF value of these individuals was approximately 2.7 (Figures 4A and 4B). In progeny of the p^M×*stony* cross, ~10.5% of the individuals with the p^M/p^M, *st/st* genotype and ~0.7 % of the individuals with the $p^M/+^{pM}$, *st/st* genotype showed a melanic color and subtle *stony* features (just very slight bulges) (Figure 4A). The body size of the p^M/p^M, *st/st* individuals were smaller than those of the p^M/_, $+^{st}$/_ individuals. They exhibited a certain sense of hardness, and the I/IF ratio was approximately 2.8, which is in good agreement with their phenotypes (Figure 4B). Additionally, individuals showing very slight melanism and morphological features that were more similar to that of the *stony* mutant (mentioned in Result 3) were all the $p^M/+^{pM}$, *st/st* genotype, and their I/IF values were

bioRxiv preprint doi: https://doi.org/10.1101/155002; this version posted June 28, 2017. The copyright holder for this preprint (which was not certified by peer review) is the author/funder, who has granted bioRxiv a license to display the preprint in perpetuity. It is made available under aCC-BY-NC-ND 4.0 International license.

approximately 1.8, which is closer to that of the *stony* mutant (Figures 4A and 4B). In addition, the expression of cuticular protein-encoding genes in p^{S}/p^{S}, *st/st* individuals were significantly higher than that in $p^{S}/+^{pS}$, *st/st* individuals (Figure. 4C); a similar result was also obtained from the p^{M}/p^{M}, *st/st* and $p^{M}/+^{pM}$, *st/st* individuals (Figure 4C). Taken together, these results revealed that more cuticular proteins with similar functions were accumulated in the cuticle of melanic homologous individuals at the *p* locus. Based on the comprehensive and association analysis, we infer that melanic background effectively drove the expressions of cuticular protein-encoding genes with similar expression patterns and redundant functions, which compensated for the morphological and adaptability defects caused by the dysfunctional *BmLcp17* gene; and the law of compensatory abilities was $p^{B}/+^{pB}$, *st/st* > p^{S}/p^{S}, *st/st* > p^{M}/p^{M}, *st/st* ≮ $p^{S}/+^{pS}$, *st/st* > $p^{M}/+^{pM}$, *st/st*, which corresponds well with the gradual weakening of the degree of melanism (Figures 4 and Figure S3).

Content variations of melanin precursors affect the transcript amount of the cuticular protein-encoding genes

Due to the crucial material basis for the cuticle melanism (no matter what kind of genetic basis caused by) is the extensive accumulation of melanin precursors in the epidermal cells; thus, the essence that melanism tend to increase the expression of some cuticular protein-encoding genes should be driven by the relations between the accumulation of melanin precursors and the transcripts amount of the cuticular protein-encoding genes. The basal expressions of four cuticular protein-encoding genes were detected in *BmNs* cells (Figure S5), indicating that there are regulatory

bioRxiv preprint doi: https://doi.org/10.1101/155002; this version posted June 28, 2017. The copyright holder for this preprint (which was not certified by peer review) is the author/funder, who has granted bioRxiv a license to display the preprint in perpetuity. It is made available under aCC-BY-NC-ND 4.0 International license.

pathways controlling the expression of cuticular protein-coding genes in this cell line; therefore, this cell line can be used to examine the effect of melanin precursors on gene expressions. After incubating *BmNs* cells with melanin precursors, the expression of cuticular protein-encoding genes was significantly higher in cells treated either by L-dopa or dopamine, compare with that in the control group (Figure 5 top (left)). In addition, when treated with BH_4, the second-instar *al* mutant (which is characterized by albinism and a porous cuticle due to a mutation of sepiapterin reductase, which leads to the insufficient synthesis of the co-factor BH_4 during the synthesis of melanin precursors (Banno *et al.* 2005; Fujii *et al.* 2013) was rescued to a melanic body color (Lab unpublished contribution) (Fujii *et al.* 2013), and the gene expressions were obviously higher than that in the control group (Figure 5 top (right)). These results suggest that the expression of cuticular protein-encoding genes can be induced by increasing amounts of melanin precursors. Furthermore, adding DAHP (an inhibitor of guanylate cyclase hydrolase (GTPCHI), which is an important rate-limiting enzyme in the synthesis of BH_4 (Hamadate *et al.* 2008), inhibited the synthesis of BH_4 in wild-type second-instar larvae by blocking the synthesis of melanin precursors in epidermal cells, which caused individuals to lose their original melanic body color (Lab unpublished contribution). The gene expressions were also significantly reduced when compared with that in the control group (Figure 5 bottom). Thus, the content and variation of the intracellular melanin precursors are important factors regulating the expression of cuticular protein-encoding genes. We concluded that the inducing effect of the melanin precursors on the expression of cuticular

bioRxiv preprint doi: https://doi.org/10.1101/155002; this version posted June 28, 2017. The copyright holder for this preprint (which was not certified by peer review) is the author/funder, who has granted bioRxiv a license to display the preprint in perpetuity. It is made available under aCC-BY-NC-ND 4.0 International license.

protein-encoding genes is the basis for melanism promoting genes‘ transcription.

Discussion

Melanin is deposited in the cuticle, in which many of cuticular proteins also occur; thus, overlapping distribution of cuticular proteins make it possible for them to interact with melanin, thereby contributing to the phenotype of the cuticle (Hopkins and Kramer 1992; Suderman *et al.* 2006; Andersen 2010; Moussian 2010; Hu *et al.* 2013). We clearly observed that extensive star-like protrusions were present on the cuticle when a large amount of melanin accumulated (Figure S1). Similar correlations between cuticle structure and body color have been reported multiple times (Futahashi *et al.* 2012; Noh *et al.* 2016; Tan *et al.* 2016), suggest that there should be some interactions between cuticular proteins and melanin. Although the exact interaction pattern between these two cuticular components is unknown, microscopic observation clearly shows that the deposition of an excessive amount of melanin affected the cuticle characteristics.

The expression profile of cuticular protein-encoding genes in melanic silkworm mutants and the black markings of *Papilio* larvae supported the view that overexpressed cuticular proteins probably participate in the transport or maintenance of the corresponding pigments in a specific painted cuticle (Figures 1, 2 and Figure S1) (Futahashi *et al.* 2012; He *et al.* 2016; Wu *et al.* 2016). Yet over-expression of cuticular protein-encoding genes *in vivo* cannot trigger (or induce) the formation of the melanic cuticle (Tajiri *et al.* 2017). Therefore, we reasoned that once the

bioRxiv preprint doi: https://doi.org/10.1101/155002; this version posted June 28, 2017. The copyright holder for this preprint (which was not certified by peer review) is the author/funder, who has granted bioRxiv a license to display the preprint in perpetuity. It is made available under aCC-BY-NC-ND 4.0 International license.

instructions for melanin accumulation are included in the developmental program (melanism being the original factor), other cuticle features and structures should adapt to the level of melanin accumulation, regardless of genetic background. The up-regulation of cuticular protein-encoding genes should be a necessary adaptation for the maintenance and stability of the structural characteristics and physical properties of melanic cuticles. The interactions of melanin and cuticular proteins at the ultrastructural level deserves special attention in follow-up studies.

Despite the elaborate regulatory mechanism by which melanin precursors affect the expression of cuticular protein-encoding genes is unclear, this study really revealed the existence of this regulatory phenomenon (Figure 5). Cuticle formation is regulated stringently in temporal and spatial patterns, the accumulation and oxidization of melanin precursors, and the interactions (such as cross-linking) among other components should occur after the formation of the initial formation of the cuticle (Moussian 2010; Sobala and Adler 2016; Tajiri 2017). Therefore, we propose that the cuticular proteins induced by melanin precursors are used to set up a platform for further accumulation and oxidization of melanin precursors. When melanin-associated protein-encoding genes have similar expression patterns and functions (Nakato *et al.* 1994; Nakato *et al.* 1997; Shofuda *et al.* 1999; Okamoto *et al.* 2008; Liang *et al.* 2010; Tang *et al.* 2010; Qiao *et al.* 2014), the production of a large amount of functionally similar cuticular proteins would be driven by the melanic background to guarantee construction and stability of the melanic cuticle. During this process, melanism unlocks the complementary features of melanin-associated cuticular proteins (such as

bioRxiv preprint doi: https://doi.org/10.1101/155002; this version posted June 28, 2017. The copyright holder for this preprint (which was not certified by peer review) is the author/funder, who has granted bioRxiv a license to display the preprint in perpetuity. It is made available under aCC-BY-NC-ND 4.0 International license.

BmLcp18, *BmLcp22*, *BmLcp30*), rescued cuticular malformation caused by the loss of function of some cuticular proteins (such as defected *BmLcp17* in *stony* mutant). Because it appears that a special cuticle-forming pattern is regulated by melanin accumulation, melanism may enhance insect adaptability to avoid the impairment of survival caused by the mutation and/or functional loss of some cuticular proteins, and these results also add new evidence to explain how melanism can be a beneficial trait (Wilson *et al.* 2001; True 2003; Wittkopp *et al.* 2003; Wittkopp and Beldade 2009; Liu *et al.* 2015; Mallet and Hoekstra 2016).

As far as we known, as structural proteins, there is no evidence to suggest that the four larval cuticular protein-encoding genes and their orthologous can enter the nucleus and regulate gene expression by acting as transcription factors. In addition, our findings and some other studies showed that changes in the expression of one cuticular protein-encoding genes of R&R family did not affect the expression of other members (Figure S6, S7) (Arakane *et al.* 2012; Noh *et al.* 2015). Moreover, several studies revealed that organisms optimize resources use at gene or protein expression level (Liebermeister *et al.* 2004; Dekel and Alon 2005); thus, the expression of melanin associated cuticle protein-encoding genes might be appropriately and simultaneously coordinated with the sufficient accumulation of intracellular melanin precursors, as a relatively direct, economical, efficient and convenient strategy. Furthermore, DAHP inhibits GTPCHI activity, but it does not directly impair the extracellular accumulation of melanin and protein–protein interactions in the cuticle. Finally, there is some evidence that melanin precursors regulate gene expressions via

bioRxiv preprint doi: https://doi.org/10.1101/155002; this version posted June 28, 2017. The copyright holder for this preprint (which was not certified by peer review) is the author/funder, who has granted bioRxiv a license to display the preprint in perpetuity. It is made available under aCC-BY-NC-ND 4.0 International license.

the receptors (Konradi *et al.* 1996; Berke *et al.* 1998; Westin *et al.* 2001). In summary, we hypothesized that the up-regulation of the four *BmLcp* genes were induced simultaneously by excessive amounts of melanin precursors, but should not be the interaction among these four genes on regulation level. To test our hypothesis, further analyses will be performed to determine the expression of the remaining *BmLcp* genes in some *BmLcps* mutant (such as defective *BmLcp17*) cell line by increasing or decreasing the content of melanin precursors.

The markings in the *stony* mutant were lighter than those in the wild-type strain, and accompanied by the down-regulation of melanin synthase genes (Figure S4). If the dysfunction of some cuticular proteins cannot be effectively supplemented, abnormalities of the cuticle structure and interactions of various cuticular components may occur, which probably result in barriers for melanin deposition and metabolism. Perhaps this is the reason why the $p^S/+^{pS}$, *st/st* (or $p^M/+^{pM}$, *st/st*) genotypes are lighter than the $p^S/+^{pS}$, $+^{st}/_$ (or $p^M/+^{pM}$, $+^{st}/_$) genotypes, besides to their different body shape. Because the homozygous of p^B mutation is lethal (Xiang 1995; Banno *et al.* 2005), we were unable to obtain F_2 progeny with the p^B/p^B, *st/st* genotype. However, it is worth noting that the body shape and the melanism degree of $p^B/+^{pB}$, $+^{st}/st$ and $p^B/+^{pB}$, *st/st* genotype individuals were almost same (Figure 4A). Therefore, during cuticle formation, if the signal promoting melanism is sufficiently strong, plenty of melanin precursors should be generated. The contents of functionally redundant proteins induced by melanin precursors are enough to fill the gap generated by the dysfunction of some cuticular proteins in theoretically, which will be able to guarantees the normal

bioRxiv preprint doi: https://doi.org/10.1101/155002; this version posted June 28, 2017. The copyright holder for this preprint (which was not certified by peer review) is the author/funder, who has granted bioRxiv a license to display the preprint in perpetuity. It is made available under aCC-BY-NC-ND 4.0 International license.

accumulation of melanin. Therefore, we believe that there should be a threshold of the melanism-promoting effect. When the accumulation of melanin precursors spans this threshold, the requirements for cuticular proteins with similar function are not weakened even when one of them loses the function, which ensuring the formation of a normal cuticle structure the later pigmentation.

We proposed a possible regulatory model as follows: when large amounts of melanin precursors induced by endogenous- and/or exogenous melanism-promoting factors, the melanin pathway may directly or indirectly induce the up-regulation of some cuticular protein-encoding genes to guarantee the formation of normal structural features of the melanic cuticle. During this process, if some cuticular proteins lose their functions, other functionally redundant cuticular proteins induced by melanin precursors can compensate for the functional defects. The compensatory intensity is increased with increasing melanin accumulation. When melanin accumulation spans a certain threshold, this compensation can totally mask the defective phenotype caused by the malfunctioning genes, which adds to growing evidence that melanism may have pleiotropic effects that enhance fitness over and above the effect of melanin accumulation itself (Figure 6). Due to the coexistence of excess melanin and cuticular proteins is common in other insects, and homologues the four *BmLcp* gene are widely distributed in the Lepidoptera (Table S2), we presume that the above reciprocal action and its corresponding biological significance are conserved in other Lepidoptera insects to that in *Bombyx mori*.

In summary, we used crucial components of the cuticle to elucidate the mutual

bioRxiv preprint doi: https://doi.org/10.1101/155002; this version posted June 28, 2017. The copyright holder for this preprint (which was not certified by peer review) is the author/funder, who has granted bioRxiv a license to display the preprint in perpetuity. It is made available under aCC-BY-NC-ND 4.0 International license.

effects among some key genetic factors, and the physiological significance of these mutual effects during the development of the morphological features. Our findings not only contribute a realistic basis to in-depth study of the interaction patterns of melanin and cuticular proteins, but they will also inspire relevant studies of other Lepidopteran insects or other insect species.

Literature Cited

Andersen, S. O., 2010 Insect cuticular sclerotization: a review. Insect Biochem Mol Biol 40**:** 166-178.

Arakane, Y., J. Lomakin, S. H. Gehrke, Y. Hiromasa, J. M. Tomich *et al.*, 2012 Formation of rigid, non-flight forewings (elytra) of a beetle requires two major cuticular proteins. PLoS Genet 8**:** e1002682.

Banno, Y., H. Fujii, Y. Kawaguchi, K. Yamamoto, K. Nishikawa *et al.*, 2005 *A guide to the silkworm mutants: 2005 gene name and gene symbol*. Kyusyu University, Fukuoka, Japan.

Berke, J. D., R. F. Paletzki, G. J. Aronson, S. E. Hyman and C. R. Gerfen, 1998 A complex program of striatal gene expression induced by dopaminergic stimulation. J Neurosci 18**:** 5301-5310.

Chaudhari, S. S., Y. Arakane, C. A. Specht, B. Moussian, D. L. Boyle *et al.*, 2011 Knickkopf protein protects and organizes chitin in the newly synthesized insect exoskeleton. P Natl Acad Sci USA 108**:** 17028-17033.

Dekel, E., and U. Alon, 2005 Optimality and evolutionary tuning of the expression level of a protein. Nature 436**:** 588-592.

Fujii, T., H. Abe, M. Kawamoto, S. Katsuma, Y. Banno *et al.*, 2013 Albino (al) is a tetrahydrobiopterin (BH_4)-deficient mutant of the silkworm *Bombyx mori*. Insect Biochem Mol Biol 43**:** 594-600.

Futahashi, R., and H. Fujiwara, 2005 Melanin-synthesis enzymes coregulate stage-specific larval cuticular markings in the swallowtail butterfly, *Papilio xuthus*. Dev Genes Evol 215**:** 519-529.

Futahashi, R., H. Shirataki, T. Narita, K. Mita and H. Fujiwara, 2012 Comprehensive microarray-based analysis for stage-specific larval camouflage pattern-associated genes in the swallowtail butterfly, *Papilio xuthus*. BMC Biol 10**:** 46.

Guan, X., B. W. Middlebrooks, S. Alexander and S. A. Wasserman, 2006 Mutation of TweedleD, a member of an unconventional cuticle protein family, alters body

bioRxiv preprint doi: https://doi.org/10.1101/155002; this version posted June 28, 2017. The copyright holder for this preprint (which was not certified by peer review) is the author/funder, who has granted bioRxiv a license to display the preprint in perpetuity. It is made available under aCC-BY-NC-ND 4.0 International license.

shape in *Drosophila*. P Natl Acad Sci USA 103**:** 16794-16799.

Hamadate, N., K. Noguchi, M. Sakanashi, T. Matsuzaki, J. Nakasone *et al.*, 2008 Effect of decreased levels of intrinsic tetrahydrobiopterin on endothelial function in anesthetized rats. J Pharmacol Sci 107**:** 49-56.

He, S. Z., X. L. Tong, K. P. Lu, Y. R. Lu, J. W. Luo *et al.*, 2016 Comparative analysis of transcriptomes among *Bombyx mori* strains and sexes reveals the genes regulating melanic morph and the related phenotypes. Plos One 11.

Hopkins, T. L., and K. J. Kramer, 1992 Insect cuticle sclerotization. Annu Rev Entomol 37**:** 273-302.

Hu, Y. G., Y. H. Shen, Z. Zhang and G. Q. Shi, 2013 Melanin and urate act to prevent ultraviolet in the integument of the silkworm, *Bombyx mori*. Arch Insect Biochem 83**:** 41-55.

Jasrapuria, S., C. A. Specht, K. J. Kramer, R. W. Beeman and S. Muthukrishnan, 2012 Gene families of cuticular proteins analogous to peritrophins (CPAPs) in *Tribolium castaneum* have diverse functions. Plos One 7.

Kanekatsu, R., Y. Banno, E. Nagashima and T. Miyashita, 1988 Genetical studies on a new spontaneous mutant "*Bamboo*" (*Bo*) of the silkworm. The Journal of Sericultural Science of Japan 57**:** 151-156.

Konradi, C., J. C. Leveque and S. E. Hyman, 1996 Amphetamine and dopamine-induced immediate early gene expression in striatal neurons depends on postsynaptic NMDA receptors and calcium. J Neurosci 16**:** 4231-4239.

Liang, J., L. Zhang, Z. Xiang and N. He, 2010 Expression profile of cuticular genes of silkworm, *Bombyx mori*. BMC Genomics 11**:** 173.

Liebermeister, W., E. Klipp, S. Schuster and R. Heinrich, 2004 A theory of optimal differential gene expression. Biosystems 76**:** 261-278.

Liu, S. S., M. Wang and X. C. Li, 2015 Pupal melanization is associated with higher fitness in *Spodoptera exigua*. Sci Rep-Uk 5.

Mallet, J., and H. E. Hoekstra, 2016 Ecological genetics: a key gene for mimicry and melanism. Curr Biol 26**:** R802-R804.

Min, C., J. B. Song, L. I. Zhi-Quan, D. M. Tang, X. L. Tong *et al.*, 2016 Progress and perspective of silkworm as a model of human diseases for drug screening. Acta Pharmaceutica Sinica.

Moussian, B., 2010 Recent advances in understanding mechanisms of insect cuticle differentiation. Insect Biochem Mol Biol 40**:** 363-375.

Moussian, B., H. Schwarz, S. Bartoszewski and C. Nusslein-Volhard, 2005 Involvement of chitin in exoskeleton morphogenesis in *Drosophila melanogaster*. J Morphol 264**:** 117-130.

Moussian, B., E. Tang, A. Tonning, S. Helms, H. Schwarz *et al.*, 2006 *Drosophila* Knickkopf and Retroactive are needed for epithelial tube growth and cuticle differentiation through their specific requirement for chitin filament organization. Development 133**:** 163-171.

Nakato, H., K. Shofuda, S. Izumi and S. Tomino, 1994 Structure and developmental expression of a larval cuticle protein gene of the silkworm, *Bombyx mori*.

bioRxiv preprint doi: https://doi.org/10.1101/155002; this version posted June 28, 2017. The copyright holder for this preprint (which was not certified by peer review) is the author/funder, who has granted bioRxiv a license to display the preprint in perpetuity. It is made available under aCC-BY-NC-ND 4.0 International license.

Biochim Biophys Acta 1218**:** 64-74.

Nakato, H., M. Takekoshi, T. Togawa, S. Izumi and S. Tomino, 1997 Purification and cDNA cloning of evolutionally conserved larval cuticle proteins of the silkworm, *Bombyx mori*. Insect Biochem Mol Biol 27**:** 701-709.

Noh, M. Y., S. Muthukrishnan, K. J. Kramer and Y. Arakane, 2015 *Tribolium castaneum* RR-1 cuticular protein TcCPR4 is required for formation of pore canals in rigid cuticle. Plos Genetics 11.

Noh, M. Y., S. Muthukrishnan, K. J. Kramer and Y. Arakane, 2016 Cuticle formation and pigmentation in beetles. Curr Opin Insect Sci 17**:** 1-9.

Okamoto, S., R. Futahashi, T. Kojima, K. Mita and H. Fujiwara, 2008 Catalogue of epidermal genes: genes expressed in the epidermis during larval molt of the silkworm *Bombyx mori*. BMC Genomics 9**:** 396.

Oota, K., and R. Kanekatsu, 1993 Morphological studies on the *Bamboo* (*Bo*) mutant of the silkworm, *Bombyx mori*. The Journal of Sericultural Science of Japan 62**:** 448-454.

Qiao, L., G. Xiong, R. X. Wang, S. Z. He, J. Chen *et al.*, 2014 Mutation of a cuticular protein, BmorCPR2, alters larval body shape and adaptability in silkworm, *Bombyx mori*. Genetics 196**:** 1103-1115.

Shofuda, K., T. Togawa, H. Nakato, S. Tomino and S. Izumi, 1999 Molecular cloning and characterization of a cDNA encoding a larval cuticle protein of *Bombyx mori*. Comp Biochem Physiol B Biochem Mol Biol 122**:** 105-109.

Sobala, L. F., and P. N. Adler, 2016 The gene expression program for the formation of wing cuticle in *Drosophila*. Plos Genetics 12.

Suderman, R. J., N. T. Dittmer, M. R. Kanost and K. J. Kramer, 2006 Model reactions for insect cuticle sclerotization: cross-linking of recombinant cuticular proteins upon their laccase-catalyzed oxidative conjugation with catechols. Insect Biochem Molec 36**:** 610-611.

Tajiri, R., 2017 Cuticle itself as a central and dynamic player in shaping cuticle. Curr Opin Insect Sci 19**:** 30-35.

Tajiri, R., N. Ogawa, H. Fujiwara and T. Kojima, 2017 Mechanical control of whole body shape by a single cuticular protein obstructor-E in *Drosophila melanogaster*. Plos Genetics 13.

Tan, D., X. L. Tong, H. Hu, S. Y. Wu, C. L. Li *et al.*, 2016 Morphological characterization and molecular mapping of an irradiation-induced Speckled mutant in the silkworm, *Bombyx mori*. Insect Mol Biol 25**:** 93-104.

Tang, L., J. Liang, Z. Zhan, Z. Xiang and N. He, 2010 Identification of the chitin-binding proteins from the larval proteins of silkworm, *Bombyx mori*. Insect Biochem Mol Biol 40**:** 228-234.

True, J. R., 2003 Insect melanism: the molecules matter. Trends Ecol Evol 18**:** 640-647.

Van Belleghem, S. M., P. Rastas, A. Papanicolaou, S. H. Martin, C. F. Arias *et al.*, 2017 Complex modular architecture around a simple toolkit of wing pattern genes. Nat Ecol Evol 1.

Wang, L.-Y., 2013 Molecular genetic studies on the oily mutants in the silkworm,

bioRxiv preprint doi: https://doi.org/10.1101/155002; this version posted June 28, 2017. The copyright holder for this preprint (which was not certified by peer review) is the author/funder, who has granted bioRxiv a license to display the preprint in perpetuity. It is made available under aCC-BY-NC-ND 4.0 International license.

Bombyx mori, pp. 43 in *Department of Agricultural and Environmental Biology, Graduate School of Agricultural and Life Sciences*. University of Tokyo.

Westin, J. E., M. Andersson, M. Lundblad and M. A. Cenci, 2001 Persistent changes in striatal gene expression induced by long-term L-DOPA treatment in a rat model of Parkinson's disease. Eur J Neurosci 14**:** 1171-1176.

Wilson, K., S. C. Cotter, A. F. Reeson and J. K. Pell, 2001 Melanism and disease resistance in insects. Ecol Lett 4**:** 637-649.

Wittkopp, P. J., and P. Beldade, 2009 Development and evolution of insect pigmentation: genetic mechanisms and the potential consequences of pleiotropy. Semin Cell Dev Biol 20**:** 65-71.

Wittkopp, P. J., S. B. Carroll and A. Kopp, 2003 Evolution in black and white: genetic control of pigment patterns in *Drosophila*. Trends Genet 19**:** 495-504.

Wu, S. Y., X. L. Tong, C. X. Peng, G. Xiong, K. P. Lu *et al.*, 2016 Comparative analysis of the integument transcriptomes of the black dilute mutant and the wild-type silkworm *Bombyx mori*. Sci Rep-Uk 6.

Xiang, Z., 1995 *Genetics and breeding of the silkworm*. Chinese Agriculture Press, Beijing, PR China.

Yoda, S., J. Yamaguchi, K. Mita, K. Yamamoto, Y. Banno *et al.*, 2014 The transcription factor Apontic-like controls diverse colouration pattern in caterpillars. Nat Commun 5**:** 4936.

Acknowledgments

We thank Dr. Tianzhu Xiong, Dr. Nathan Edelman, Dr. Jorge Eduardo Amaya Romero and Ms. Yan Yao for the valuable advices. This work was supported by the Hi-Tech Research and Development 863 Program of China (Grant No. 2013AA102507), the National Natural Science Foundation of China (No. 31302038; 31372379), the Natural Science Foundation Project of ChongQing (CSTC) (No. cstc2013jcyjA80022) and Par-Eu Scholars Program (20136666).

Figure legends

Figure 1. Expression of four larval cuticular protein-encoding genes in melanic and non-melanic integuments. A and B represent the gene expressions between the

bioRxiv preprint doi: https://doi.org/10.1101/155002; this version posted June 28, 2017. The copyright holder for this preprint (which was not certified by peer review) is the author/funder, who has granted bioRxiv a license to display the preprint in perpetuity. It is made available under aCC-BY-NC-ND 4.0 International license.

semi-lunar marking (black box) and the non-melanic region (between the semi-lunar marking, red box) in Dazao or Dazao-*stony*, respectively. Scale bar: 2 mm. C. Comparative analysis of gene expressions in the dorsal side of abdominal segments (from the third to the fourth segment, red box) between the p^S and Dazao strains. Scale bar: 1 cm. D. Comparison of gene expressions between the second-instar *al* mutant and the Dazao strain (melanic). The red hashtag symbol indicates the Fig. 1 D we are showing is cited from the previous study of our lab group (Min *et al*. 2016) with modification. Scale bar: 2 mm. *t*-test, n=3; * $p < 0.05$; ** $p < 0.01$; *** $p < 0.001$.

Figure 2. Expression of cuticular protein-encoding genes in integuments showing different degree of melanism. A and B display comparisons of degree of melanism and cuticular protein-encoding gene expression levels among four strains with mutant alleles at the *p* locus. Scale bar: 1 cm. Ratios represent the ratios of gene expression levels between two strains. Symbols (−, +, ++, and +++) represent the increment of the degree of melanism. Star represents the melanin-associated cuticular protein-encoding genes. *t*-test, n=3; * $p < 0.05$; ** $p < 0.01$.

Figure 3. Segregation patterns of the phenotypes of progenies from different crosses of melanic mutant strains and the *stony* strain. In the segregated progenies, the first item in the list (B,N), (B,st), (S,N), (S,st), (M,N), (M,st), (N,N) and (N,st) represents p^B-, p^S- p^M- and Normal color patterns, respectively. The second item indicates body

bioRxiv preprint doi: https://doi.org/10.1101/155002; this version posted June 28, 2017. The copyright holder for this preprint (which was not certified by peer review) is the author/funder, who has granted bioRxiv a license to display the preprint in perpetuity. It is made available under aCC-BY-NC-ND 4.0 International license.

shape features marked with non-*stony* type (N) and the *stony* type (st). It is noteworthy that in (S, st-am+) and (M, st-am+), the second item represents the ambiguous *stony* body shape. The size of "+" symbol represents the corresponding degree of the ambiguous *stony* body shape. Superscript "T"s represent theoretical values. Superscript "A"s represent actual values. Backslashes indicates that a value was not obtained. Chi-squared test, * $p < 0.05$; ** $p < 0.01$.

Figure 4. Association analysis of the genotypes, phenotypes and gene expression levels in segregated progenies from different crosses. A. Correlation analysis between the genotypes and phenotypes in self-crossed or backcrossed progenies. Scale bar: 1 cm. White and red stars represent polymorphic bands at the $+^{p}$ and p^{X} loci ($X = B$, S or M), respectively. Red and white hash-tag represent polymorphic bands at the *st* and $+^{st}$ locus, respectively. Solid and dotted red arrows indicate the relative degree of bulging (solid > dotted), respectively. Slashes show the genotypes within one phenotypic category. The thickness of the slash represents the proportion of the corresponding genotypes. Dotted backslashes indicate that the number of individuals with the corresponding genotype is quite low. B. Ratios of the length of internodes and intersegmental folds in the second, third, and fourth abdominal segments of individuals with different genotypes (showing melanic body color) in the self-crossed or backcrossed progenies. n≥3, *t*-test, ** $p < 0.01$. C. Gene expression analysis of cuticular protein-encoding genes in homogeneous and heterogeneous individuals at the *p* locus from self-crossed progenies of p^{S} × *stony*, and p^{M} × *stony* under the

bioRxiv preprint doi: https://doi.org/10.1101/155002; this version posted June 28, 2017. The copyright holder for this preprint (which was not certified by peer review) is the author/funder, who has granted bioRxiv a license to display the preprint in perpetuity. It is made available under aCC-BY-NC-ND 4.0 International license.

condition that the cuticle was melanic and the genotype was homozygous recessive at *st* locus. n = 3, *t* – test, * $p < 0.05$; ** $p \leq 0.01$.

Figure 5. Effect of melanin precursors (top left: in cells) and BH_4 (top right: in *vivo*) treatments on the expression of cuticular protein-enconding genes (*t*-test; n = 3, * $p < 0.05$; ** $p < 0.01$), and variations of gene expression levels in larval cuticle treated with the inhibitor DAHP (bottom). n = 3, *t*-test, ** $p < 0.01$.

Figure 6. Schematic overview of the effect of melanin precursors on the expressions of cuticular protein-encoding genes. Black solid circles represent the melanin. Triangles represent the BmLcps with similar expression patterns and functions. Solid and hollow triangles represent the normal and defective functions, respectively. Red rhombi represent other components (such as chitin) in the cuticle. Solid and dotted double-headed arrows indicate probable interactions and loss of interactions due to the functional deficiency of some *BmLcps* (such as dysfunctional *BmLcp17*), respectively. Purple arrows show the direction in which the melanin precursors or cuticular proteins flow from the haemolymph to the epidermal cells as well as from the epidermal cells to the cuticle. Red arrows indicate the increased contents of melanin precursors or the up-regulation of cuticular protein-encoding genes. Purple polyline arrows indicate melanism-promoting factors produced by other genetic instructions. Double dovetail arrows indicate the effect of melanin precursors on cuticular protein-encoding genes. The question mark indicates that the details of

bioRxiv preprint doi: https://doi.org/10.1101/155002; this version posted June 28, 2017. The copyright holder for this preprint (which was not certified by peer review) is the author/funder, who has granted bioRxiv a license to display the preprint in perpetuity. It is made available under aCC-BY-NC-ND 4.0 International license.

induction (directly or indirectly) are unclear. Here the cuticle especially means the exo-cuticles in which the melanin and cuticular proteins deposited in (Hopkins and Kramer 1992; Suderman *et al.* 2006; Andersen 2010; Moussian 2010).

Figure 1

bioRxiv preprint doi: https://doi.org/10.1101/155002; this version posted June 28, 2017. The copyright holder for this preprint (which was not certified by peer review) is the author/funder, who has granted bioRxiv a license to display the preprint in perpetuity. It is made available under aCC-BY-NC-ND 4.0 International license.

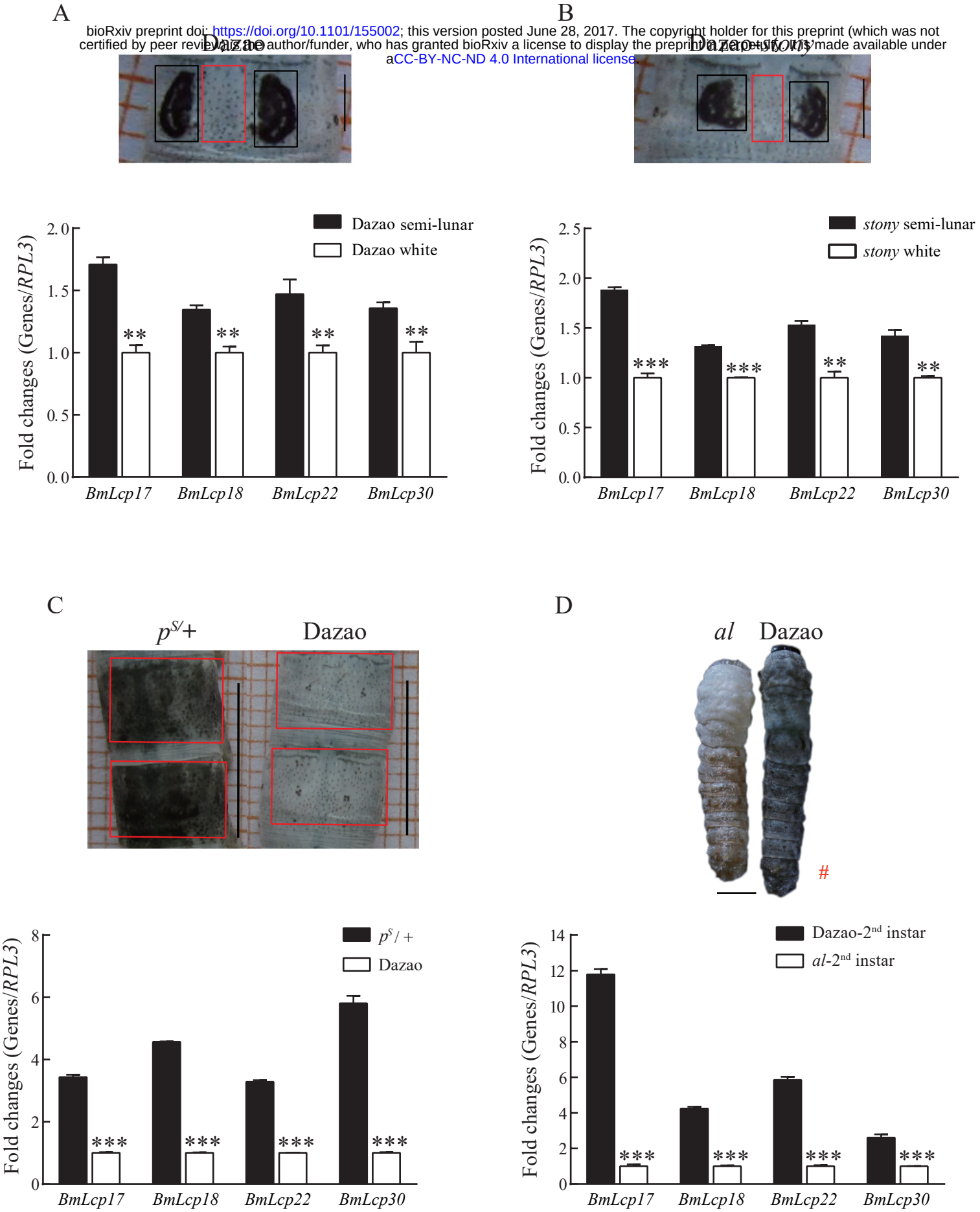

Figure 2

bioRxiv preprint doi: https://doi.org/10.1101/155002; this version posted June 28, 2017. The copyright holder for this preprint (which was not certified by peer review) is the author/funder, who has granted bioRxiv a license to display the preprint in perpetuity. It is made available under aCC-BY-NC-ND 4.0 International license.

A

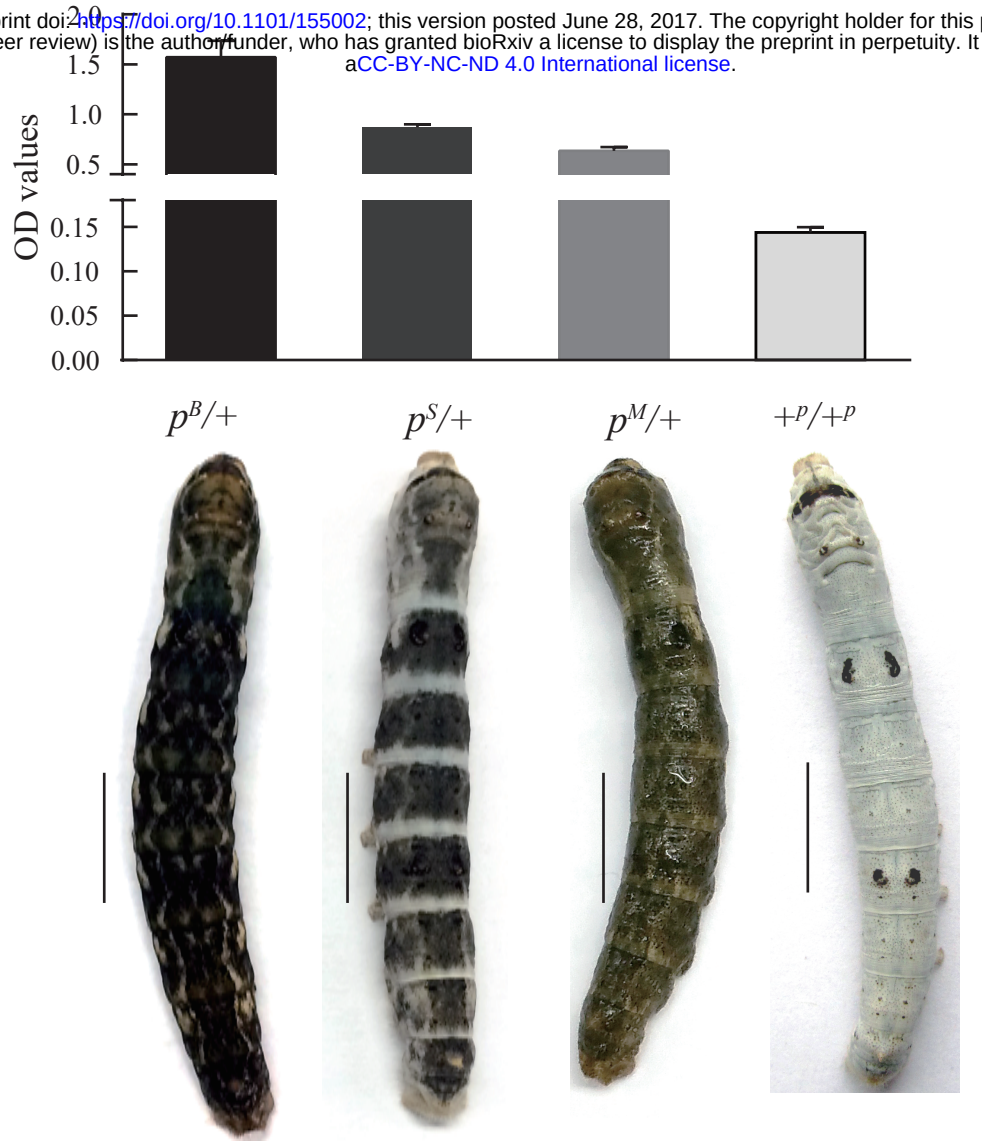

B

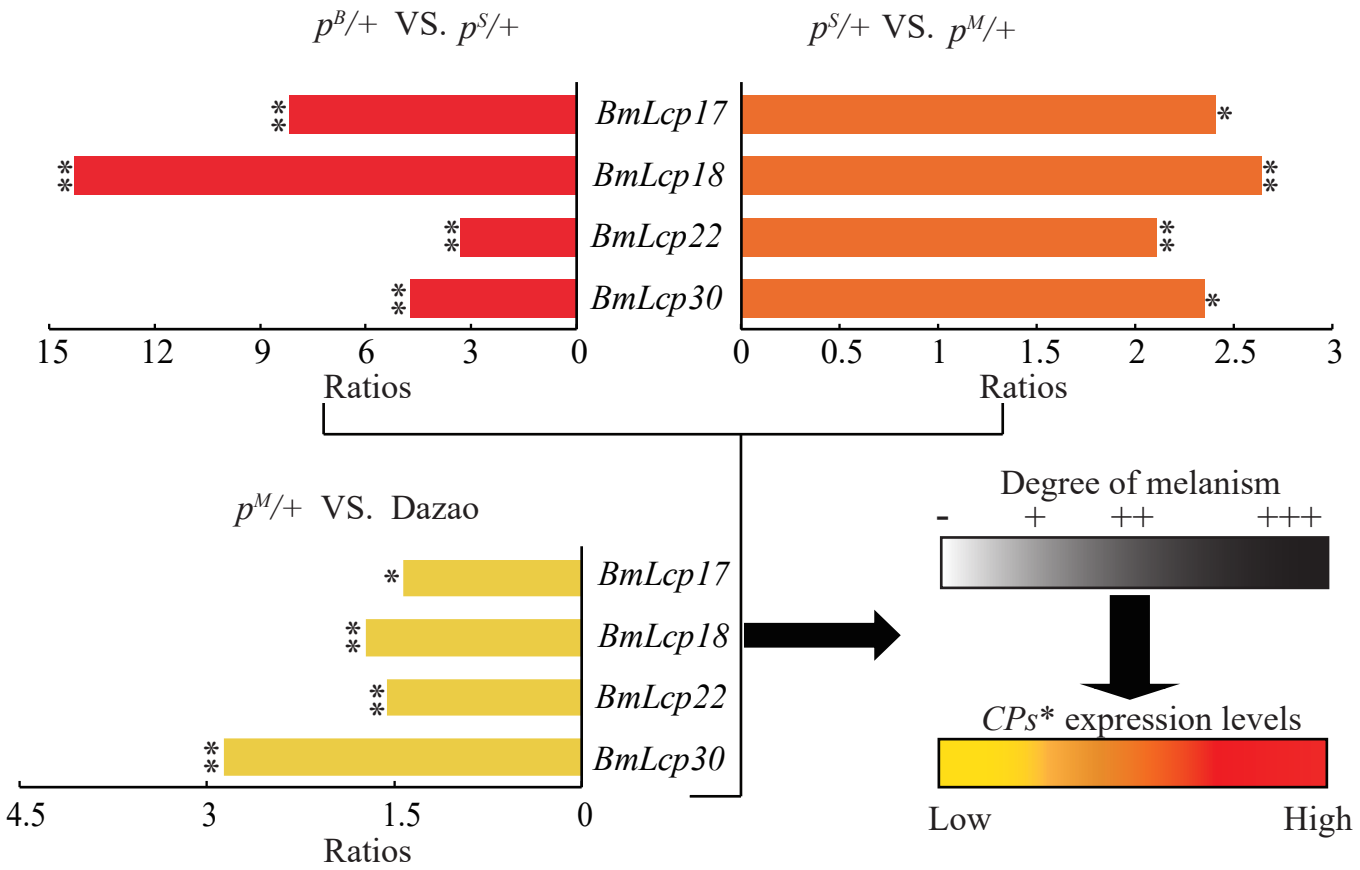

Figure 3

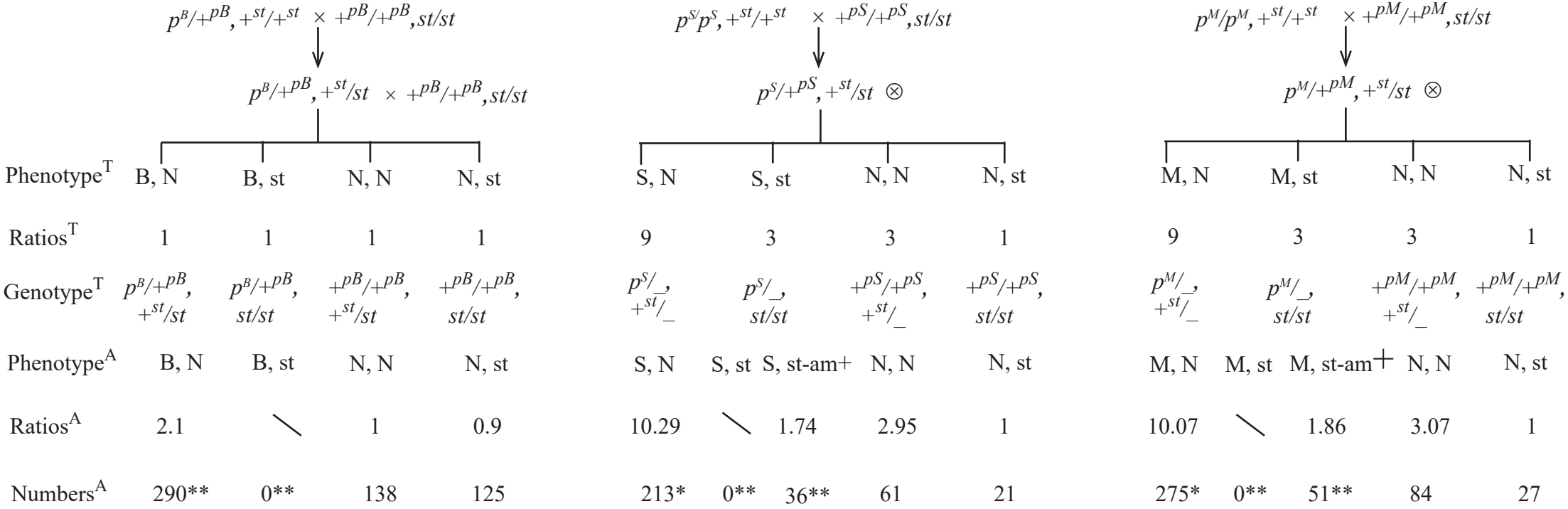
$p^B/+^{pB}, +^{st}/+^{st} \times +^{pB}/+^{pB}, st/st$
$p^B/+^{pB}, +^{st}/st \times +^{pB}/+^{pB}, st/st$
$p^S/p^S, +^{st}/+^{st} \times +^{pS}/+^{pS}, st/st$
$p^S/+^{pS}, +^{st}/st \otimes$
$p^M/p^M, +^{st}/+^{st} \times +^{pM}/+^{pM}, st/st$
$p^M/+^{pM}, +^{st}/st \otimes$
Phenotype^T B, N B, st N, N N, st S, N S, st N, N N, st M, N M, st N, N N, st
Ratios^T 1 1 1 1 9 3 3 1 9 3 3 1
Genotype^T $p^B/+^{pB}, +^{st}/st$ $p^B/+^{pB}, st/st$ $+^{pB}/+^{pB}, +^{st}/st$ $+^{pB}/+^{pB}, st/st$ $p^S/_, +^{st}/_$ $p^S/_, st/st$ $+^{pS}/+^{pS}, +^{st}/_$ $+^{pS}/+^{pS}, st/st$ $p^M/_, +^{st}/_$ $p^M/_, st/st$ $+^{pM}/+^{pM}, +^{st}/_$ $+^{pM}/+^{pM}, st/st$
Phenotype^A B, N B, st N, N N, st S, N S, st S, st-am+ N, N N, st M, N M, st M, st-am+ N, N N, st
Ratios^A 2.1 \ 1 0.9 10.29 \ 1.74 2.95 1 10.07 \ 1.86 3.07 1
Numbers^A 290** 0** 138 125 213* 0** 36** 61 21 275* 0** 51** 84 27

Figure 4

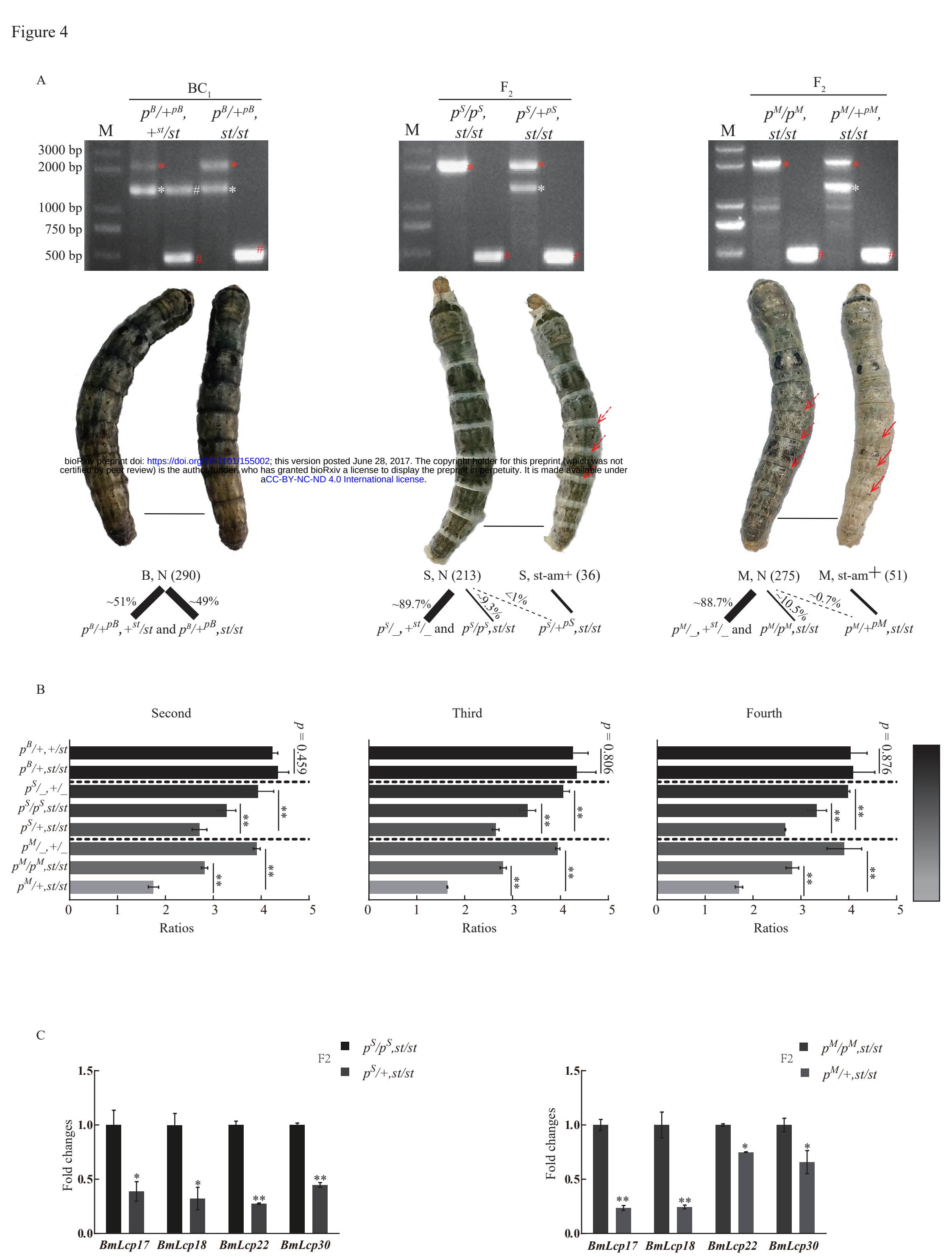

bioRxiv preprint doi: https://doi.org/10.1101/155002; this version posted June 28, 2017. The copyright holder for this preprint (which was not certified by peer review) is the author/funder, who has granted bioRxiv a license to display the preprint in perpetuity. It is made available under aCC-BY-NC-ND 4.0 International license.

Figure 5

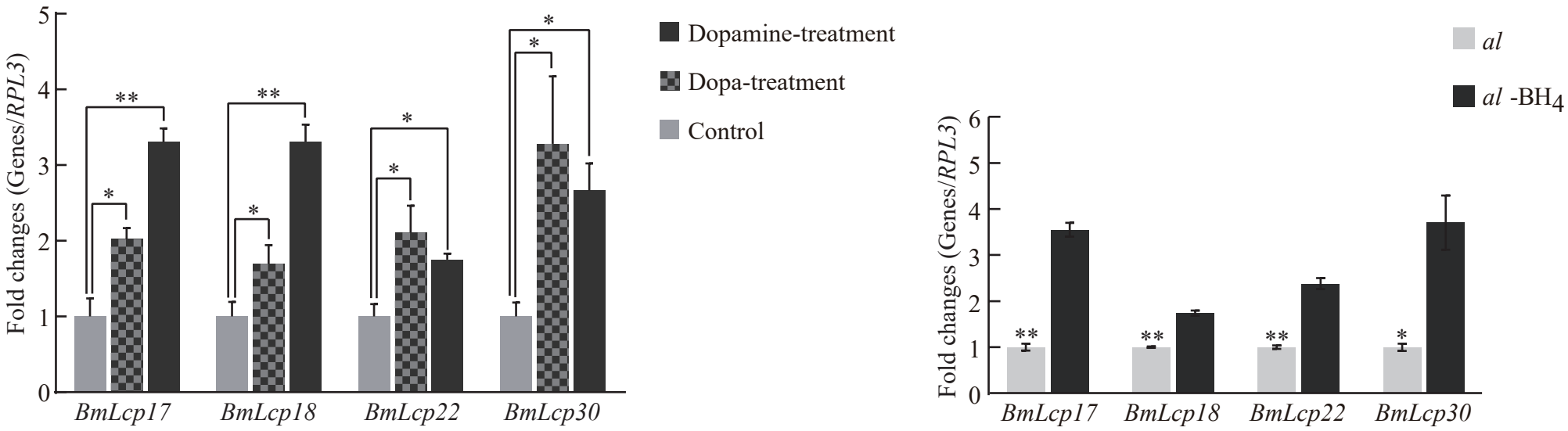

bioRxiv preprint doi: https://doi.org/10.1101/155002; this version posted June 28, 2017. The copyright holder for this preprint (which was not certified by peer review) is the author/funder, who has granted bioRxiv a license to display the preprint in perpetuity. It is made available under aCC-BY-NC-ND 4.0 International license.

Contents of melanin precursors

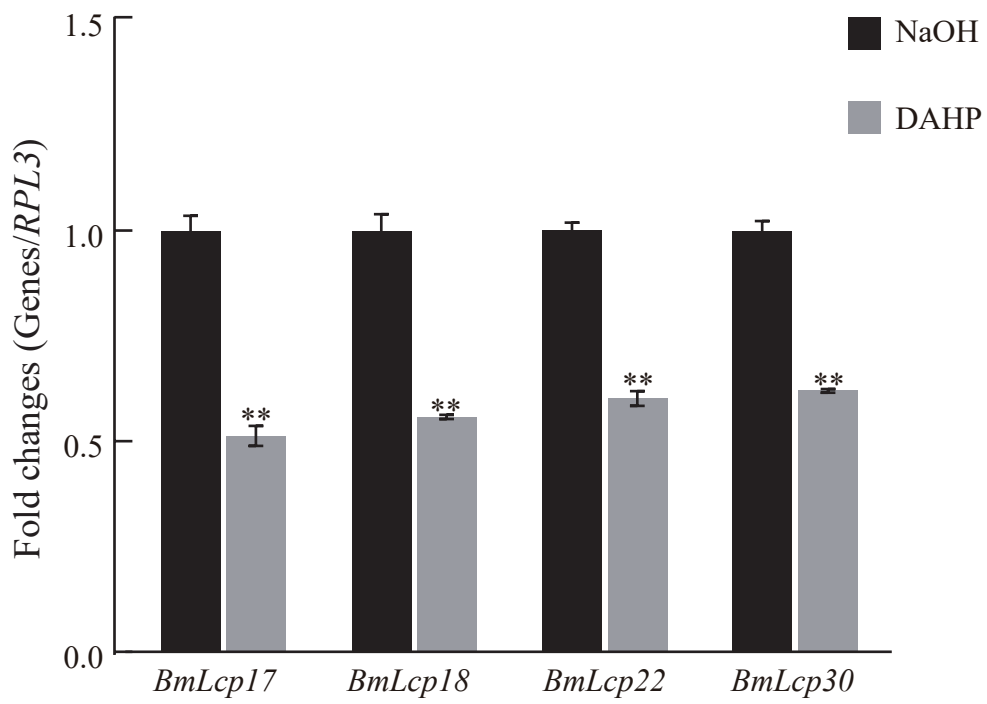

Figure 6
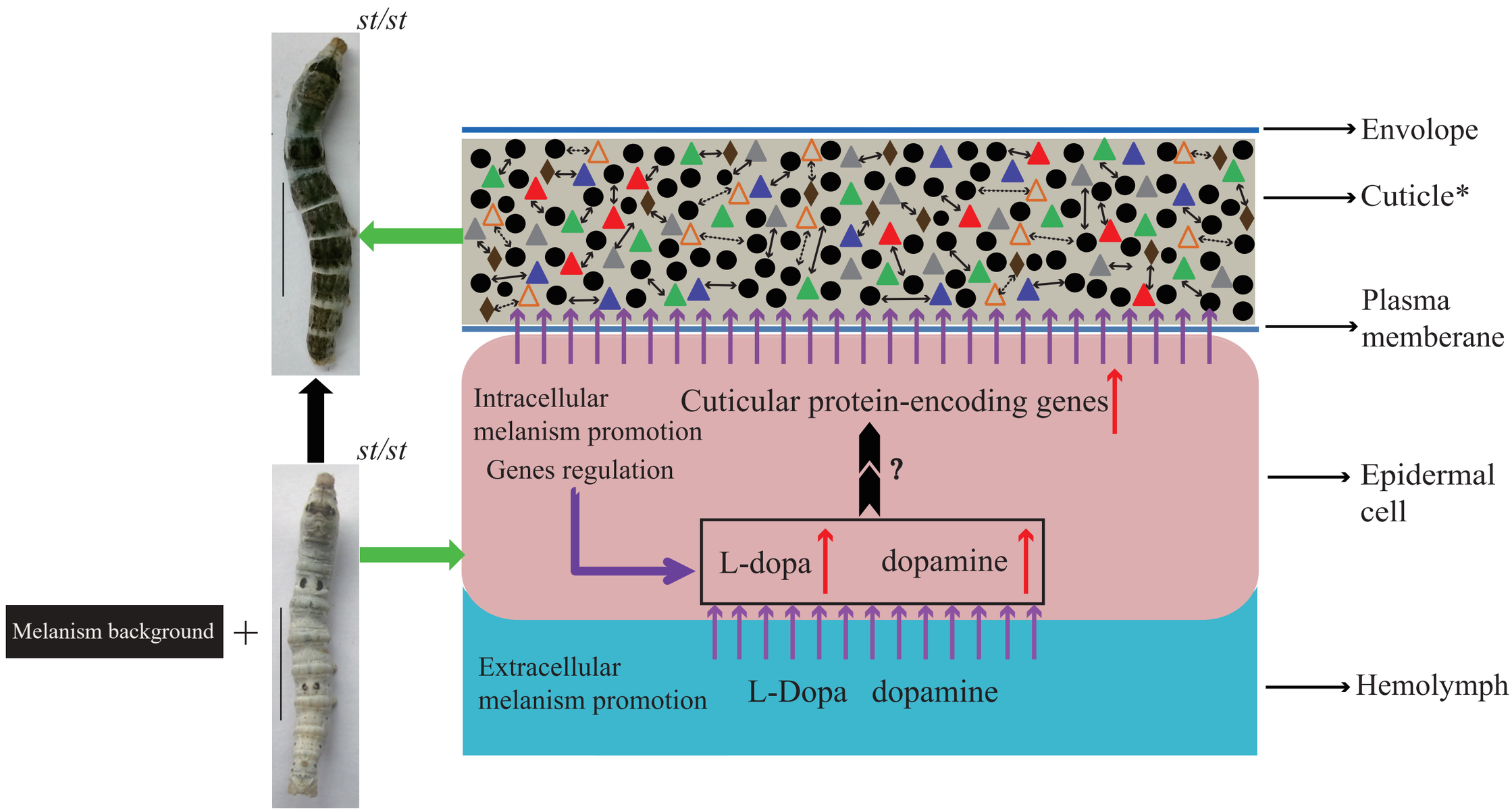
bioRxiv preprint doi: https://doi.org/10.1101/155002; this version posted June 28, 2017. The copyright holder for this preprint (which was not certified by peer review) is the author/funder, who has granted bioRxiv a license to display the preprint in perpetuity. It is made available under aCC-BY-NC-ND 4.0 International license.